The Giant Organelles in *Beige* and Chediak-Higashi Fibroblasts Are Derived from Late Endosomes and Mature Lysosomes

By Janis K. Burkhardt, Frederike A. Wiebel, Susan Hester, and Yair Argon

From the Department of Immunology, Duke Medical Center, Durham, North Carolina 27710

Summary

Chediak-Higashi Syndrome (CHS) is an autosomal recessive disease affecting secretory granules and lysosome-like organelles. In CHS fibroblasts, acidic organelles are abnormally large and clustered in the perinuclear area. We have analyzed fibroblast cell lines from a CHS patient and from the murine model for CHS, the *beige* mouse, to determine which lysosome-like compartments are affected. Uptake of neutral red showed that in both *beige* and CHS cell lines, the acidic organelles were markedly clustered in the perinuclear region of the cells. Giant organelles (>4 μm) were observed in a fraction of the cells, and these were more dramatic in the *beige* fibroblasts than in the CHS fibroblasts. The total dye uptake of both mutant cell lines was similar to their respective wild type fibroblasts, suggesting that the overall volume of acidic compartments is unaffected by the disorder. Histochemistry and immunofluorescence showed that the giant organelles in both *beige* and CHS fibroblasts were positive for cathepsin D, lysosome-associated membrane protein (LAMP) 1, LAMP 2, and a 120-kD lysosomal glycoprotein, all marker proteins for late endosomes and lysosomes. The giant organelles were also negative for transferrin receptor and mannose-6-phosphate receptor, and most of them were also negative for rab 7. This distribution of marker proteins shows that the giant organelles in both *beige* and CHS are derived from late compartments of the endocytic pathway. This conclusion was confirmed using endocytic tracers. BSA was transported to the giant organelles, but only after long incubation times, and only at 37°C. α_2-Macroglobulin was taken up and degraded at similar rates by CHS or *beige* cells and their respective wild type control cells. Taken together, our results indicate that the mutation in CHS specifically affects late endosomes and lysosomes, with little or no effect on early endosomes. Although the mutation clearly causes mislocalization of these organelles, it appears to have little effect on their endocytic and degradative functions.

Chediak-Higashi Syndrome (CHS)[1] is a rare autosomal recessive disorder in humans, affecting multiple cell lineages and commonly classified as a lysosomal abnormality (1). Analogous disorders have been identified in a variety of species (2–4), the best studied of which is the *beige* mouse (5, 6). CHS patients suffer from dilution of skin pigmentation, severe recurrent infections, lymphoproliferative disorder and progressive peripheral neuropathy, reflecting the range of affected cells (7). Many of the clinical manifestations can be attributed to abnormalities in leukocyte function, and several hemopoietic lineages, including neutrophils and cytolytic lymphocytes, have been shown to be functionally defective in CHS and in *beige* (8–13).

At the cellular level CHS is characterized by the presence of giant organelles. There is, however, considerable diversity and tissue specificity in the nature of these giant organelles; secretory organelles are enlarged in some cell types while endocytic organelles are affected in others (6, 8, 12). Neutrophils, platelets, eosinophils, mast cells, and cytolytic lymphocytes from CHS patients, all cells that normally engage in regulated secretion, contain massive secretory granules. In each case, the enlarged secretory granule retains its characteristic ultrastructure and protein composition. In nonsecretory cell types, such as monocytes and fibroblasts, the enlarged organelles are lysosome-like. Thus, the histological classification of CHS betrays a complex range of affected cellular organelles.

The giant organelles in CHS and *beige* cells are often described as lysosomes, but this definition is largely based on classical histochemical criteria (6, 8). In recent years, how-

[1] *Abbreviations used in this paper:* CD-MPR, cation-dependent (46 kD) mannose-6-phosphate receptor; CHS, Chediak-Higashi syndrome; CI-MPR, cation-independent (300 kD) mannose-6-phosphate receptor; DTAF, dichlorotirazinylamino-fluorescein; LAMP, lysosome-associated membrane protein; lgp-120, 120-kD lysosomal glycoprotein; α_2M, α_2-macroglobulin; NM1, normal mouse 1.

 J. Exp. Med. © The Rockefeller University Press • 0022-1007/93/12/1845/12 $2.00
Volume 178 December 1993 1845–1856

ever, it has become apparent that the "lysosomotropic" dyes that stain the giant organelles, such as neutral red and acridine orange, are not exclusive markers for lysosomes. It is now known that coated and uncoated vesicles, early endosomes, late endosomes, and lysosomes are all acidified to varying degrees and therefore all can accumulate these dyes (14). Similarly, acid phosphatase, a "lysosomal marker" found in the giant organelles, is known to have a broader intracellular distribution (15, 16).

Recent work on the endocytic pathway has resulted in the characterization of several marker proteins that distinguish more definitively among distinct endocytic compartments. Several membrane spanning proteins are now known to reside in some but not all of the endocytic compartments. The transferrin receptor cycles between the plasma membrane and early endosomes (17); the cation-independent and cation-dependent mannose-6-phosphate receptors (CI- and CD-MPR) are found in late endosomes but not in mature lysosomes (18), whereas the lysosome-associated membrane proteins (LAMPs) and 120-kD lysosomal glycoprotein (lgp-120) (19, 20) reside in both late endosomes and lysosomes. Much has also been learned about how both soluble lysosomal enzymes and membrane-spanning glycoproteins are targeted to lysosomes, and conditions have been defined that block movement between endocytic compartments (21, 22). Finally, small GTP binding proteins from the rab family have been shown to be involved in vesicle fusion along the endocytic pathway and to interact specifically with distinct endocytic compartments (23). In light of all this new information, it was interesting to ask more precisely whether the CHS and *beige* mutations affect a defined endocytic compartment, and if so, whether the same compartment is affected in both humans and mice.

Recent clinical advances in treating CHS patients center around bone marrow transplantation, replacing only hemopoietic cells. As survival times of patients increase, understanding the effects of the CHS defect on other cells will be important for predicting and treating abnormalities in other tissues. Therefore, in this study we focused on defining the defect in fibroblasts. By better understanding which endocytic compartments are affected in these cells, we seek to develop a unifying explanation for the effects of the disease on endocytic organelles and secretory granules in various cell types.

Materials and Methods

Cells. GM02075A is a skin fibroblast cell line, derived from an 18-mo-old female with clinical symptoms of Chediak-Higashi Syndrome, and was obtained from the Human Genetic Mutant Cell Repository (Camden, NJ). The human control skin fibroblast line, CCD-45Sk, was derived from a 3-mo-old female, and obtained from the American Type Culture Center (Rockville, MD). The *beige* and normal mouse (NM1) lines were derived from C57BL/6J-Bg^J and C57BL/6J mice, respectively (24), a generous gift of Dr. T. Lyerla (Clark University, Worcester, MA). CCD-45Sk and GM02075A were maintained in Dulbecco's minimal essential medium supplemented with nonessential amino acids and 10–15% FCS (both from JRH Biosciences, Lenexa, KS), while the murine lines were maintained in Dulbecco's minimal essential medium supplemented with 5% FCS.

Antibodies. Antibody to the lysosomal glycoprotein lgp-120 was a gift of Dr. I. Mellman (Yale University, New Haven, CT); 1D4B monoclonal anti-mouse LAMP1 and ABL-93 anti-mouse LAMP 2 (20) were originally produced by Dr. T. August (Johns Hopkins University, Baltimore, MD) and obtained from the Developmental Studies Hybridoma Bank; rabbit anti-human LAMP1/2 antibody was a kind gift of Dr. M. Fukuda (La Jolla Research Foundation, La Jolla, CA); rabbit anti-cathepsin D sera were gifts of Dr. J. Mort (McGill University, Montreal, Canada) and Dr. K. von Figura (University of Gottingen, Germany); anti-MPR antisera were gifts of Dr. W. Brown (Cornell University, Ithaca, NY) and Dr. B. Hoflack (EMBL, Heidelberg, Germany). Rabbit anti-rab 7 and monoclonal anti-rab 5 were gifts of Dr. M. Zerial (EMBL, Heidelberg, Germany). Mouse mAb B3/25 anti-human transferrin receptor was purchased from Boehringer Mannheim Corp., Indianapolis, IN. The secondary antibodies used were: FITC-goat anti-rabbit IgG (Sigma Chemical Co., St. Louis, MO); Texas red- and FITC-goat anti-rat IgG (Jackson ImmunoResearch Labs, West Grove, PA, and Rockland Inc., Gilbertsville, PA); Texas red- and Cy3-donkey anti-rabbit Ig (Jackson Labs); and FITC-goat anti-mouse IgG (Southern Biotechnology, Birmingham, AL).

Light Microscopy. Immunofluorescence studies were performed as described previously (25). Briefly, cells grown on coverslips were fixed with 2% paraformaldehyde/PBS, quenched with 50 mM NH_4Cl/PBS and permeabilized with PBS/0.01% saponin/0.25% gelatin (PSG). Coverslips were incubated for 1 h with primary antibodies diluted appropriately in PSG, washed six times with PSG, incubated 1 h with secondary antibody, and washed six times. Localization of rab proteins was performed essentially as described in (23). Cells were permeabilized before fixation by a 5-min incubation with 0.03% saponin/80 mM Pipes, pH 7.2/1 mM $MgCl_2$/5 mM EGTA, and then fixed with 2% paraformaldehyde in PBS. Coverslips were mounted in 10% glycerol/PBS/2.5% diazabicyclo-(2,2,2)octane, and observed using an Axiovert microscope (Zeiss, Oberkochen, Germany) with a MRC-600 laser confocal attachment (Bio-Rad Inc., Richmond, CA). Acid phosphatase cytochemistry was performed using the Sigma (St. Louis, MO) kit according to the manufacturer's instructions, and visualized using brightfield optics.

Uptake Studies. For neutral red staining, cells grown on coverslips were incubated for 30 min with 20–200 μM neutral red in PBS, washed three times rapidly in PBS, mounted in PBS, and observed under phase contrast. For quantitation of neutral red uptake, the cells were lysed in 1% Triton X-100/0.1 M HCl (26) and the amount of dye was determined spectrophotometrically.

For fluorescence uptake studies, BSA was conjugated to dichlorotriazinylamino-fluorescein (DTAF). The molar ratio of DTAF-BSA in the conjugate was 5–6:1. Cells were incubated with 5 mg/ml DTAF-BSA in complete medium for various times at 20°C or 37°C, fixed, and either viewed directly, or processed as described above for double-label immunofluorescence.

Electron Microscopy. BSA was conjugated to 12 nm gold particles (27), and fed to cells for various times at 37°C. The cells were fixed on the Petri dish with 2% glutaraldehyde/0.15 M sodium cacodylate, pH 7.4, 1 mM $CaCl_2$, scraped, and processed for electron microscopy as described previously (28), except that no staining was done after sectioning.

Immunoblots. Cells were washed three times with balanced salt solution and then lysed with buffer containing 1% NP-40 (25). Nuclei were pelleted and the postnuclear supernatants were subjected to SDS-PAGE. After electrophoresis, the total cellular proteins were transferred onto a nitrocellulose membrane (Amersham Corp., Arlington Heights, IL) using a Hoefer apparatus and probed

with antibodies as described previously (29). The anti-human LAMP1/2 antibody was used at 1:500 dilution and developed using ^{125}I-protein A (Amersham Corp.).

Uptake and Degradation of α_2-Macroglobulin. Purified α_2-macroglobulin (α_2M) was a generous gift of Drs. G. Salveson and J. Enghild (from the Dept. of Pathology, Duke University, Durham, NC). The protein was treated with methylamine as in (30) to convert it to the receptor-binding form, iodinated with the IodoBead reagent (Pierce, Rockford, IL), and repurified by gel filtration. The sp act was 9,000 cpm/ng. Binding of ^{125}I-α_2M to the cells was completely inhibited by 100× excess of unlabeled α_2M. The uptake studies were performed using the method of Maxfield et al. (31). Duplicate 35-mm plates of cells (grown to subconfluency) were deprived of serum for 1 h, allowed to bind ^{125}I-α_2M at 4°C for 1 h, washed at 4°C and then incubated for various times at either 4°C, 20°C, or 37°C. At the end of each time point, medium and cells were separated, the cells were washed three times with cold buffer, and then lysed with 0.5% NP-40 in PBS. The TCA soluble and precipitable cpm in each sample were then determined, to calculate the extent of α_2M degradation.

Results

Acidic Organelles Are Abnormally Distributed. The structural abnormality in *beige* cells and in CHS cells is commonly detected by visualizing the uptake of the dye neutral red, which accumulates in acidic intracellular compartments. As shown in Fig. 1 *B*, uptake of neutral red by fibroblasts from a mouse homozygous for the *beige* mutation reveals a pattern that is quite different from that observed with normal mouse fibroblasts. First, in comparison with normal fibroblasts, where a significant number of neutral red-positive organelles are scattered throughout the periphery (Fig. 1 *A*), the neutral-red positive organelles in *beige* cells are much more clustered in the perinuclear region and are almost completely excluded from peripheral extensions (Fig. 1 *B*, arrowheads). Second, there is a dramatic variation in size of the neutral red-positive vesicles in *beige* fibroblasts. In addition to the normal-sized structures, several giant organelles (3–4 μm in diameter) can be found in many cells. In normal fibroblasts the size distribution of the neutral red-positive vesicles is much narrower, and giant ones are seen only very rarely. Though the appearance of the giant vesicles is the most dramatic aspect of the *beige* phenotype, there is considerable cell-to-cell variation in the number and size of the giant organelles. Furthermore, we noticed that after prolonged incubation with neutral red the size of the giant organelles increases. The perinuclear clustering of all the neutral red-positive structures seems to be a more consistent aspect of the *beige* phenotype (e.g., 2, 6).

A similar phenotype is displayed by fibroblasts derived from a CHS-patient (Fig. 1 *D*). By comparison with a matched line of normal human fibroblasts (Fig. 1 *C*), the neutral red-positive vesicles in the CHS fibroblasts are strongly concentrated near the nucleus, and are virtually excluded from peripheral extensions of the cell (Fig. 1 *D*, arrowheads). In addition, the average size of the acidic organelles is larger than in the control cells. At least in the fibroblast line used in this study, the appearance of exceptionally large organelles (Fig. 1 *D*, arrow) was relatively rare; the clustered distribution and a moderate size increase were more characteristic of the CHS cells.

It is clear from the distribution of neutral red in the *beige* and CHS cells that both mutations result in the formation of acidic organelles that are fewer in number and larger than normal. We therefore compared the total cellular uptake of neutral red in the two mutant cell lines with that of their matched control lines. Cells that had been incubated with neutral red for 30 min were washed briefly, lysed in acidic detergent solution (26), and their dye content measured spectrophotometrically. The total dye uptake by CHS and *beige* cells was remarkably similar to that of their respective control cell lines (Table 1). The total uptake of neutral red should

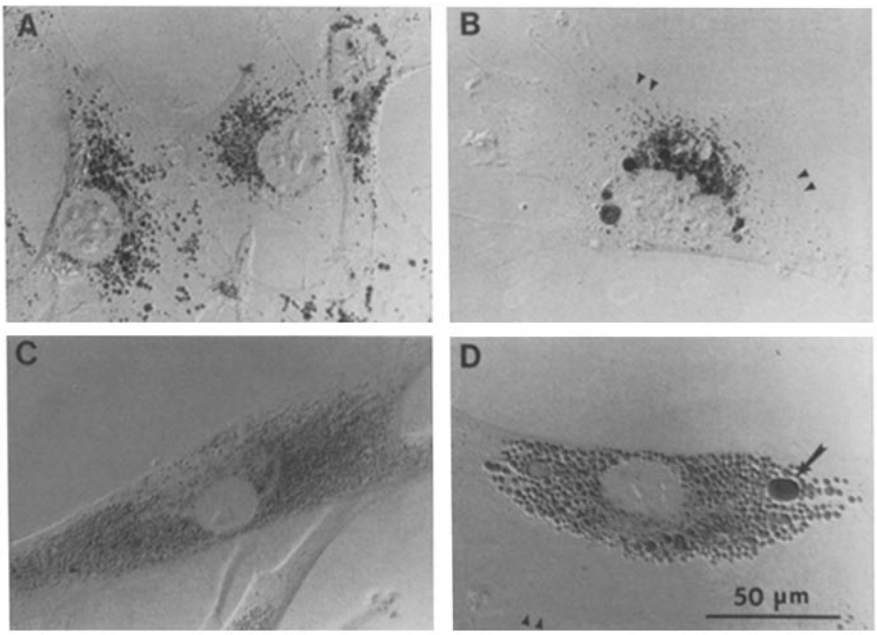

Figure 1. Neutral red uptake by fibroblast cell lines. Normal murine fibroblasts (*A*), *beige* murine fibroblasts (*B*), normal human fibroblasts (*C*) and CHS human fibroblasts (*D*) were incubated with neutral red for 30 min and viewed with DIC optics. Note the perinuclear clustering and size variability of neutral red-positive organelles in *B* and *D* as compared with *A* and *C*, respectively. Arrowheads in *B* and *D* point to the cell boundaries. (*Arrow*) A giant neutral red-positive organelle.

Table 1. *Quantitation of Neutral Red Uptake by Fibroblasts*

Cell	$A_{550}/10^6$ cells*	n‡	Neutral red/ cell
			fmol
Beige	4.187 ± 2.748	5	108 ± 71
NM1	3.810 ± 1.469	4	100 ± 39
CHS	3.144 ± 0.809	4	75 ± 19
CCD	3.250 ± 1.896	4	78 ± 43

* Uptake studies were performed with either 20 or 200 μM input neutral red. OD measurements were normalized to the lower input values, since both concentrations were found to be in the linear range of uptake.
‡ Number of separate experiments, each performed on triplicate plates.

be proportional to the product of the total volume of acidic compartments accessible to the dye and the acidity of those compartments. In T lymphocytes, where we have used the DAMP method (32) to determine the pH of individual lysosomes and endosomes, the *beige* mutation showed no effect on the pH of either organelle (Hester, S., J. Burkhardt and Y. Argon, unpublished data). Assuming that the same is true in *beige* and CHS fibroblasts, we surmise that the comparable uptake of neutral red by the fibroblasts reflects comparable overall volumes of the endosomal/lysosomal compartments. Taken together, the results with neutral red show that the acidic compartments in *beige* and CHS fibroblasts are normal in pH and volume, but abnormal in their intracellular distribution.

The Giant Organelles Contain Markers for Late Endocytic Compartments. Since neutral red is taken up by many acidic or-

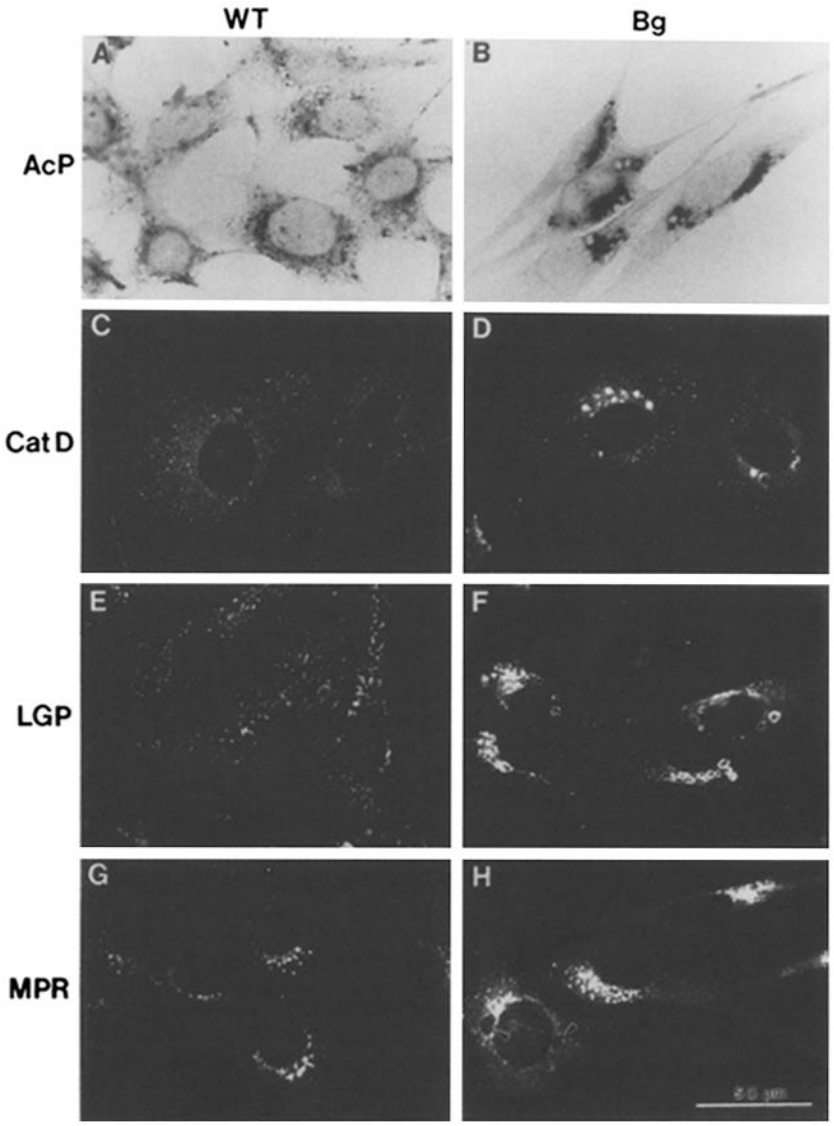

Figure 2. Distribution of lysosomal and endosomal marker proteins in *beige* cells. Acid phosphatase (AcP) was detected histochemically and observed using bright field optics. Cathepsin D (CatD), (LGP-120), and the cation-independent mannose-6-phosphatase receptor (MPR) were detected by confocal immunofluorescence microscopy, as described in Materials and Methods.

ganelles, we used specific marker proteins to determine more precisely which compartments are affected in the *beige* and CHS fibroblasts. Acid phosphatase, a hydrolase present in lysosomes and in endosomes, was detected histochemically (Fig. 2, *A* and *B*). Most of the acid phosphatase-positive vesicles were tightly clustered in the perinuclear region in *beige* cells, whereas in normal fibroblasts they could be seen in peripheral processes. In the *beige* cells, numerous giant organelles were acid phosphatase positive. Similar staining of clustered organelles was obtained in the CHS fibroblasts (Fig. 3 *B*) as compared with control human cells (Fig. 3 *A*). Cathepsin D, an endosomal/lysosomal hydrolase, which unlike acid phosphatase (16) bears the mannose-6-phosphate lysosomal targeting signal, was localized by confocal immunofluorescence microscopy. Although the anti–cathepsin D antibody labeled small peripheral structures in addition to the giant organelles, it was clear that the compartment affected by *beige* and CHS contains this hydrolase (Figs. 2, *C-D*, and 3, *C–D*).

Because these hydrolases reside in both endosomes and lysosomes, we examined the distribution of membrane glycoproteins that have been used to distinguish between endosomes and lysosomes (33). The cation-independent mannose-6-phosphatase receptor (CI-MPR) is present in early and late endosomes, but is absent from mature lysosomes (18). In contrast, members of the LAMP family of lysosomal glycoproteins, including LAMP1/lgp120 and LAMP2, are present in late endosomes and lysosomes but absent from early endosomes (19, 20, 34). As shown in Figs. 2 *F* and 3 *F*, the giant vesicles were LAMP-positive in both CHS and *beige* fibroblasts. Importantly, in both mutants the giant vesicles were negative for CI-MPR (Figs. 2, *G-H* and 3, *G–H*). Indeed, they sometimes appeared as "negatively stained" structures, made visible by the surrounding MPR-positive endosomes (Fig. 2 *H*, arrowheads). These results were confirmed using four independent antibodies to the LAMP family of proteins, and three separate anti-CI-MPR antibodies (not shown).

The distribution of two small GTP binding proteins was also examined as a means of identifying the defective com-

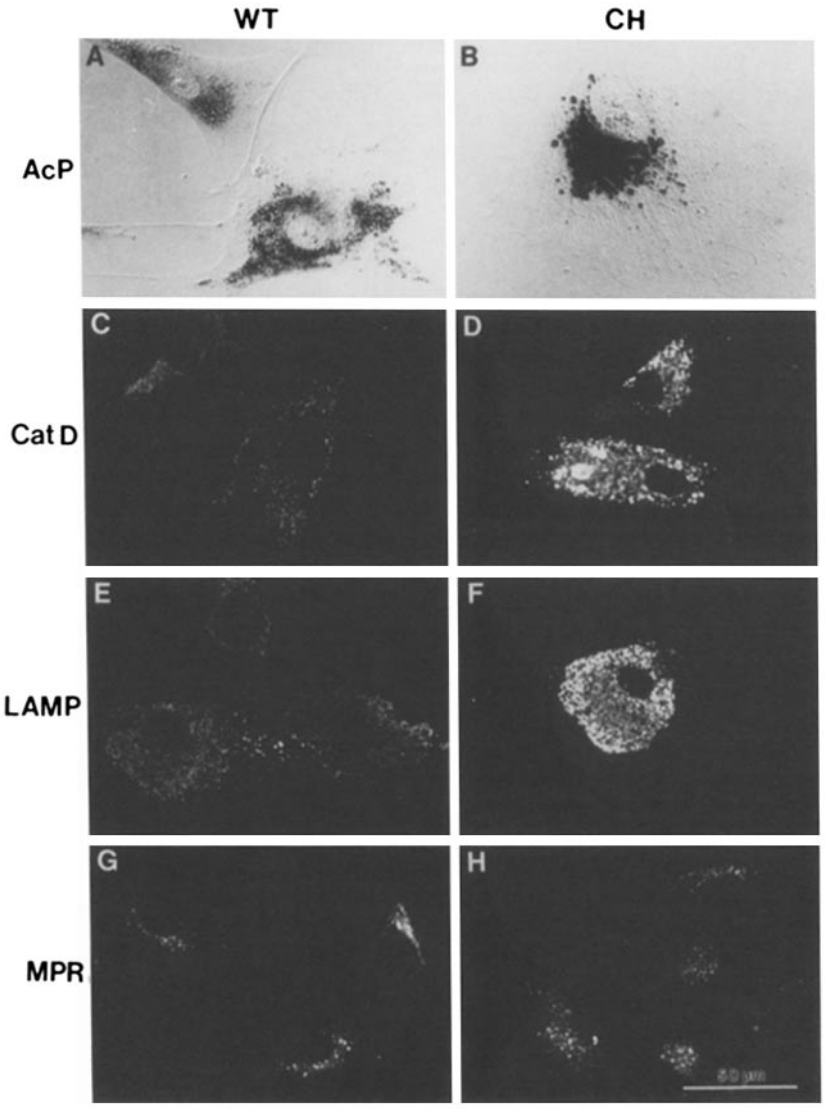

Figure 3. Distribution of lysosomal and endosomal marker proteins in CHS cells. The same histochemical assay and antibodies as described in legend to Fig. 2 were used on CHS and normal human fibroblasts, with the substitution of the anti–human LAMP1/2 (LAMP) antibody as a lysosomal membrane glycoprotein marker.

partment. Rab 5 and rab 7 have been shown to bind to early and late endosomal compartments, respectively (35, 36, 23). When the distribution of these proteins was examined in the *beige* and CHS fibroblasts, anti-rab 5 antibody did not stain the giant perinuclear organelles (data not shown). In contrast, anti-rab 7 antibody did label some giant organelles, as well as other smaller structures (Fig. 4). When double label immunofluorescence was performed on normal mouse cells, the distribution of rab 7 (Fig. 4 *B*) was a subset of the distribution of LAMP-1 (Fig. 4 *A*). This is in keeping with the late endosomal localization of rab 7 in other cell types (35, 36, 23). In *beige* cells, some of the large LAMP-positive structures were positive for rab 7 (Fig. 4, *C–D*, arrow), whereas most were negative (Fig. 4, *C–D*, arrowheads). Single labeling of the human cells with anti-rab 7 revealed occasional giant organelles and a clustered distribution in the CHS cells (Fig. 4 *F*) relative to wild type controls (Fig. 4 *E*).

Finally, we tested the distribution of the transferrin receptor as another criterion to distinguish between early and late endosomes. Anti-transferrin receptor antibody gave a fine punctate labeling pattern on all the cells tested. The giant organelles were consistently negative for this marker of early endosomes (data not shown).

The presence of the hydrolases and lysosomal membrane proteins in the giant organelles indicates that these structures derive from late endosomal or lysosomal compartments. The markers that usually distinguish late endosomes from lysosomes, MPR, and rab 7, give somewhat conflicting results. The absence of CI-MPR from the giant organelles defines them as mature lysosomes, but the presence of rab 7 on at least some giant organelles marks these as more similar to the late endosomal compartment.

The CHS Mutation Does Not Affect the Total Amount of LAMP Family Proteins. The marker analysis showed that the LAMP glycoproteins were the best markers for the clustered giant organelles in both CHS and *beige* cells. The staining with these antibodies was almost completely restricted to the affected compartment. The fluorescence intensity was very strong in the mutant cells with each of the anti-LAMP antibodies tested, raising the possibility that these proteins are overexpressed in *beige* and CHS cells. Western blot analysis was performed to test this possibility. Lysates were prepared from CHS and control cells, and equivalent amounts of lysate were compared by SDS-PAGE and immuno-blotting with a rabbit serum that recognizes LAMPs 1 and 2 in human cells (20). Similar levels of LAMP glycoproteins were detected in CHS and control cell lines (Fig. 5). Therefore, the apparent increase in immunofluorescence intensity with antibodies to LAMP family proteins must be due to concentration of these proteins in the perinuclear region and the increased size of the organelles, but not due to overexpression of these proteins.

The Giant Organelles Function As Late Endocytic Compartments. Are the defective lysosomes/late endosomes still capable of receiving endocytosed material, or are they off-

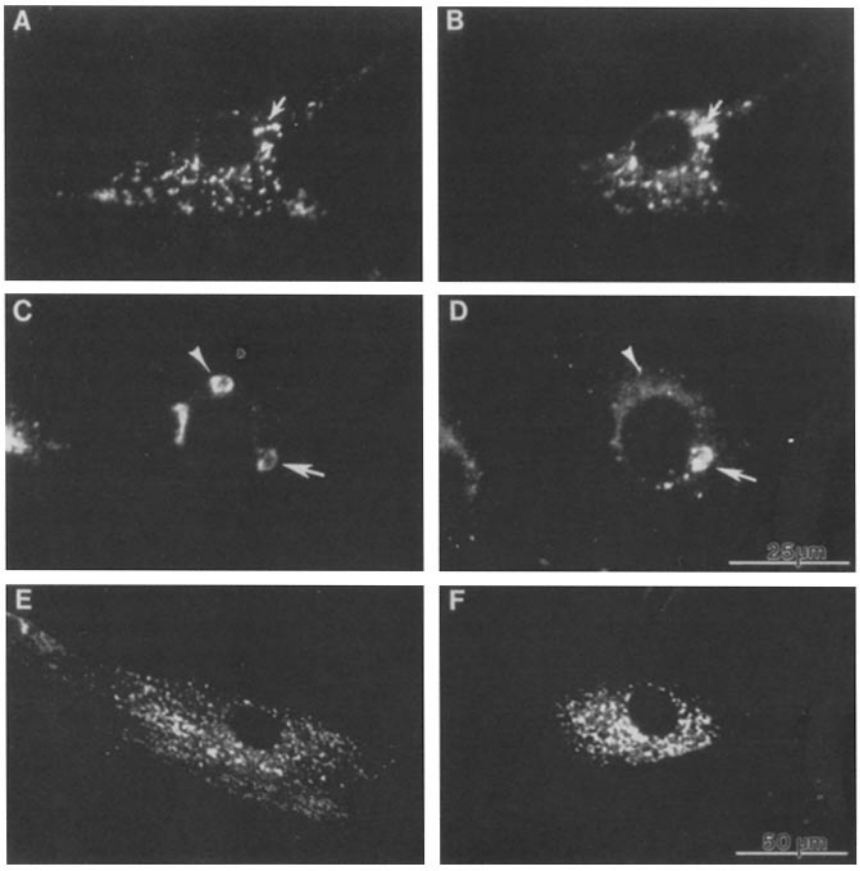

Figure 4. Distribution of rab 7, a marker for late endosomes. *A* and *B*, wild type mouse fibroblasts. *C* and *D*, *beige* fibroblasts. Each pair shows cells doubly labeled with anti-LAMP1 (rat MAb 1D4B) followed by Texas red goat anti-rat Ig (*A* and *C*), and with rabbit anti-rab 7 followed by FITC goat anti-rabbit Ig (*B* and *D*). The arrows in *A* and *B* point to typical vesicular structures in the wild type cells that are positive for both markers. The arrows in *C* and *D* show a giant organelle that is double labeled, whereas the arrowheads show a giant organelle that lacks rab 7. (*E*) Normal human fibroblasts labeled with anti-rab 7 followed by FITC goat anti-rabbit Ig; note the disperse distribution. (*F*) CHS fibroblasts labeled similarly; note the clustered distribution.

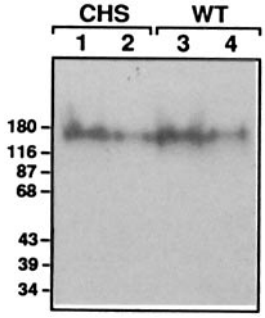

Figure 5. Comparison of LAMP protein levels in CHS and normal cells. Total detergent lysates from CHS or control fibroblasts were fractionated by SDS-PAGE, transferred onto nitrocellulose membrane, and probed with rabbit anti-human LAMP1/2 serum, followed by ^{125}I-protein A. (Lanes *1* and *3*) Lysates from 3 × 10^5 cells. (Lanes *2* and *4*) Lysates from 1 × 10^5 cells. The mobilities of marker proteins are indicated at left.

pathway aberrant structures? To address this question, *beige* cells were incubated with DTAF-conjugated BSA for 3 h at 37°C, chased overnight to load the lysosomal compartment (37), and then fixed and counter-labeled with anti-lgp120 to mark the giant organelles. When viewed by confocal microscopy, the DTAF-BSA had accumulated in various-sized vesicles, including giant perinuclear structures (Fig. 6 *A*) that were rimmed with lgp120 (Fig. 6 *B*). DTAF-BSA could be detected in the giant organelles after 2.5 h of continuous uptake, but the intensity of fluorescence increased with longer incubation times, up to 6 h of uptake or more. This finding was verified by electron microscopy of BSA-colloidal gold uptake by *beige* cells (Fig. 7). After 20 min of uptake at 37°C, BSA-gold particles were found in small (<0.4 μm in diameter) endosomal vesicles, both in the cell periphery and in the perinuclear region (not shown). After 4 h of continuous uptake, some BSA-gold particles were still located in these small

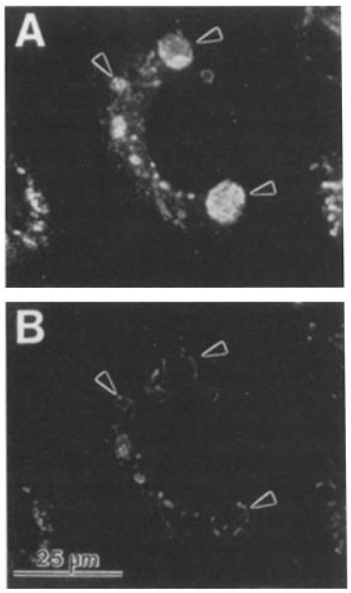

Figure 6. Uptake of fluorescent BSA into the giant organelles of *beige* cells. A representative *beige* cell doubly labeled with endocytosed DTAF-BSA and anti-lgp120. *Beige* cells were incubated with DTAF-BSA for 3 h at 37°C, and chased overnight. They were subsequently fixed and counter-labeled with rat anti-lgp120 followed by Texas red goat anti-rat Ig. (*A*) DTAF-BSA. (*B*) anti-lgp120. Arrowheads point to giant organelles filled with BSA which also show membrane distribution of lgp120.

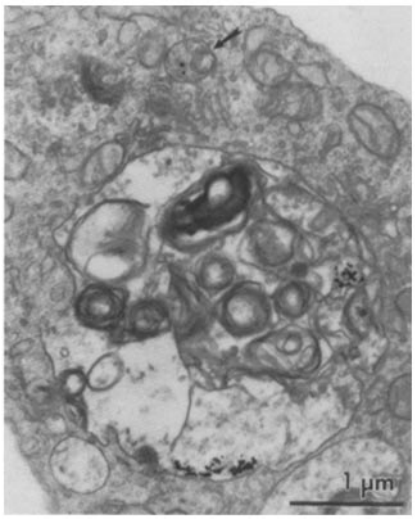

Figure 7. Electron microscopy of BSA uptake into the giant organelles of *beige* cells. Profile of a *beige* cell after 4 h of uptake of colloidal gold-BSA. Note the multivesicular ultrastructure of the giant organelle. (*Arrow*) A small endosome, typical of the BSA containing structures found also after 20 min of uptake.

early endosomes (Fig. 7, arrow) while others had reached the giant perinuclear bodies (up to 4 μm in diameter; Fig. 7). These pleiomorphic organelles contained membranous whorls and other material, and their structure was consistent with that reported by others (1, 38, 39). BSA-gold first appeared in these giant organelles between 60 and 120 min of uptake, consistent with transport to late endosomes and lysosomes.

Incubation at 20°C has been shown to block transport of internalized material from early endosomes into late endosomes and lysosomes (22). When *beige* and CHS fibroblasts were incubated with DTAF-BSA at 20°C instead of 37°C, the tracer did not reach the giant organelles. Instead, the DTAF-BSA remained in smaller, more dispersed structures (Fig. 8). By this operational criterion the giant organelles function as late endocytic compartments. The distribution of DTAF-BSA at 20°C was the same as in the wild type control cells (not shown), indicating that there are no gross functional abnormalities in early endosomes of CHS and *beige* cells.

Taken together, these studies show that the giant clustered organelles in *beige* and CHS cells are still active in endocytic traffic of exogenous ligands, and are therefore on-pathway structures. Traffic to the affected compartment is somewhat slowed, but overall, it has the properties expected for traffic to late endosomes and lysosomes.

The Mutant Cells Take Up and Degrade an Exogenous Ligand Normally. To quantify the receptor-mediated uptake and degradation of an exogenous ligand in the CHS and *beige* cells we used iodinated α_2-macroglobulin (α_2M). This serum protein binds, in a complex with proteases, to a surface receptor present on fibroblasts, and their endocytic route has been studied extensively (31). ^{125}I-α_2M was bound to the cells at 4°C and then chased at 37°C for various times. As

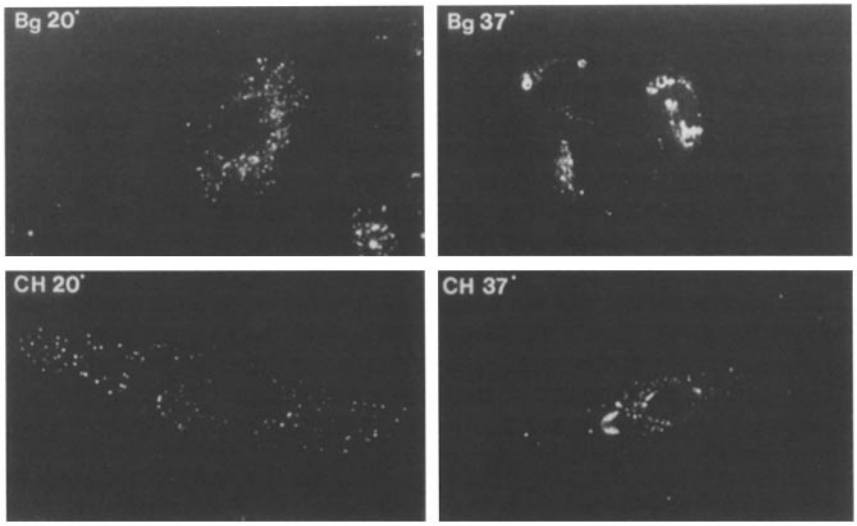

Figure 8. Effect of reduced temperature on arrival of endocytosed BSA at the giant organelles. *Beige* or CHS cells were viewed after continuous uptake of DTAF-BSA for 3–4 h at either 20°C or 37°C. Note that at 20°C DTAF-BSA is limited to small endocytic vesicles throughout the cytoplasm and is absent from the giant organelles.

compared with their normal counterparts, CHS and *beige* cells bound similar amounts of α_2M and internalized similar amounts over a 4-h time course (data not shown). α_2M degradation was measured as the appearance of TCA soluble counts in both the cell lysates and the media. Both *beige* and CHS cells were capable of degrading the internalized α_2M, with neither mutant showing dramatic defects in comparison to its matched control line (Fig. 9 *A*). Within individual experiments, a small decrease in the extent of α_2M degradation was consistently observed in the *beige* cells, but this difference was small relative to the variation among experiments. To determine what portion of the measured degradation occurred in early and late endocytic compartments, cells were allowed to internalize bound α_2M for 3 h at either 20°C or 37°C. In both mutant and control cell lines, degradation was blocked at 20°C (Fig. 9 *B*), indicating the requirement for transport to late endocytic compartments, presumably including the giant organelles.

Discussion

One main finding of this study is that the abnormally enlarged vesicles commonly observed in fibroblasts from both *beige* mice and human patients with CHS are derived from the late organelles of the endocytic pathway: mature secondary lysosomes and late endosomes. Previous reports had described the giant structures as "lysosomes" because they take up neutral red and endocytic tracers and contain acid phosphatase (e.g., [6, 8]), or because they lack specific lysosomal enzymes (39a). However, these criteria do not distinguish among the various compartments along the endocytic pathway. In this study we used more precise markers and functional criteria to show that the giant organelles are late endocytic compartments.

It is clear from our studies that early endosomal compartments are not affected in either CHS or *beige*. First, transferrin receptor and rab 5, proteins found on the plasma membrane and early endosomes, are not found on the giant organelles. CI-MPR, which marks the same early endosomes as well as later endosomes, is also missing from the defective organelles. Second, DTAF-BSA does not appear in abnormally large structures until late times of uptake, and at 20°C, where movement between early and late endosomes is blocked, the transfer of BSA to the giant organelles is blocked.

Marker analysis and functional studies both indicate that the defects in CHS and *beige* are in late endocytic compartments. The giant organelles contain acid phosphatase and cathepsin D, hydrolases which are targeted by independent mechanisms to late endosomes and lysosomes (16). In addition, the defective compartment contains much of the cells' lysosomal membrane glycoproteins (LAMP1/lgp-120 and LAMP2). These glycoproteins are present in both late endosomes and mature lysosomes, but are not present to any appreciable extent in earlier endocytic compartments (40, 19, 20, 34). The properties of tracer uptake are also characteristic of late endocytic compartments. The kinetics of uptake into the giant organelles and the sensitivity to reduced temperature are similar to those found for transport into late endosomes and lysosomes in wild type cells.

It is difficult to determine to what degree the CHS and *beige* mutations selectively affect late endosomes vs. lysosomes. Functional studies provide no clues, since conditions have not been found that block exchange of material between the two compartments, and since late endosomes are active in degradation of proteins (41). By electron microscopy, the giant organelles resemble the complex membranous structure of late endosomes more than the dense, spherical structure of lysosomes. Marker proteins that are usually used to classify the late endosomes and lysosomes give a somewhat mixed picture. The giant organelles were negative for CI-MPR, as expected for mature lysosomes, but some of them were positive for rab 7, which is a marker protein for late endosomes. It is, of course, possible that the mutations cause selective mislocalization of either CI-MPR or rab 7. In this context, it should also be noted that the presence of CI-MPR in certain late endosomal/lysosomal structures is somewhat variable. For example, phagolysosomes in macrophages sometimes

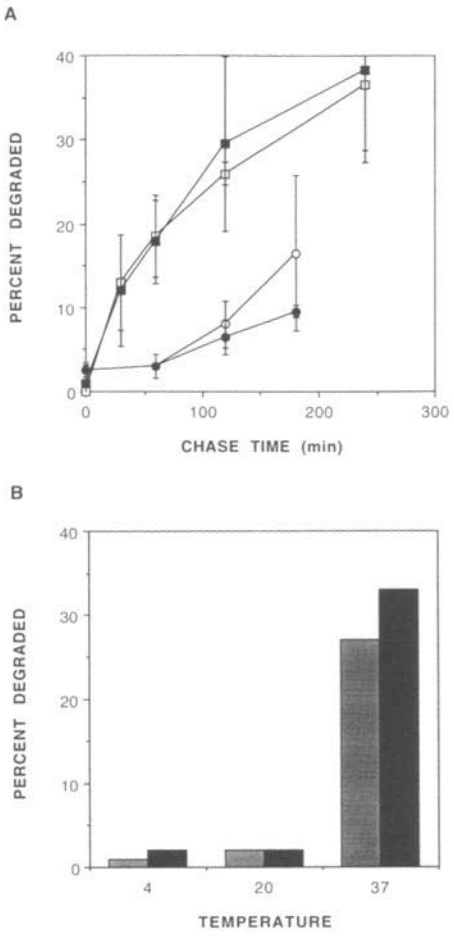

Figure 9. Degradation of α_2M by *beige* and CHS cells. (*A*) Kinetics of degradation. Plates of cells were pulsed with ^{125}I-α_2M at 4°C for 1 h, washed extensively to remove unbound ligand, and then incubated for various times at 37°C. At the end of each chase time point, medium, and cells were separated, and the TCA soluble and precipitable radioactivity in each was determined. The percentage of the initial cell-bound radioactivity which was converted to TCA soluble radioactivity is shown. The results are expressed as means ± SE, derived from three–five independent experiments with each of the four cell lines. *Beige* fibroblasts (*filled squares*). Wild type mouse fibroblasts (*open squares*). CHS fibroblasts (*filled circles*). Wild type human fibroblasts (*open circles*). (*B*) Temperature dependence of α_2M degradation. *Beige* or wild type cells were pulsed with ^{125}I-α_2M for 1 h at 4°C, washed, and then incubated for 3 h at either 4°C, 20°C, or 37°C. The percentages of TCA soluble radioactivity at each temperature are shown. *Beige* (*dotted bars*). Wild type (*filled bars*).

contain CI-MPR (42) and sometimes lack both it and the cation-dependent MPR (43). In cytolytic lymphocytes that contain late endosome–like lytic granules, these lytic granules sometimes contain (8) and sometimes lack (44) CI-MPR, and the distribution of CI-MPR changes with the differentiation of these lymphocytes (Griffiths, G., S. Hester, J. Burkhardt, and Y. Argon, manuscript in preparation). Such cases preclude total reliance on the available markers and illustrate the need for further criteria to distinguish between late endosomes and lysosomes.

The appearance of the giant organelles is superficially reminiscent of the selective "swelling" of this compartment in the presence of sucrose or other nondigestible carbohydrates (45). Though the mechanism of giant organelle formation in CHS is not known and in fact is often attributed to excessive fusion (46, 47), the selective effect of the mutation, like the selective effect of sucrose loading on late endocytic compartments, underscores biochemical differences that must exist between lysosomes and endosomes despite the many common features of these endocytic compartments.

A second main conclusion of this study is that despite their structural abnormality, the giant organelles are part of the normal endocytic pathway. Exogenous ligands which enter the cell either by fluid phase endocytosis (BSA), bulk membrane retrieval (cationized ferritin; data not shown), or receptor-mediated endocytosis (α_2M) all reach the giant lysosomes/late endosomes of the mutant fibroblasts. The uptake into the giant vesicles is slow, however; more than 6 h are required for substantial accumulation in this compartment as compared to 3–4 h in wild type cells. Interestingly, neither the *beige* mutation nor the CHS lesion impairs the cells' protein catabolic activity. The α_2M employed as ligand here is typical of proteins that are taken up and degraded efficiently in lysosomes (31). In our hands, α_2M degradation occurred only at 37°C, both in normal and in mutant fibroblasts, indicating that degradation required transport to a late endocytic compartment. In the CHS cells, the degradation of α_2M was detectable only after more than 2 h of endocytosis, but in *beige* significant degradation was measured already after 60 min. The extent of α_2M degradation we measured agrees well with the degradation of α-glucosidase by CHS cells as measured by Miller et al. (48). It should be pointed out that since there is considerable heterogeneity of late endosomal/lysosomal organelles in both CHS and *beige* cells, it is possible that most of the degradation occurs in unaffected organelles, either late endosomes or small normal lysosomes. However, our studies with the various tracers indicate that a significant proportion of endocytosed material is transported to the giant organelles. Therefore, it is more likely that they either function normally or equilibrate with a functional catabolic compartment.

The normal catabolic activity of late endocytic compartments in CHS and *beige* is consistent with the observation that these organelles maintain a constant volume. In this respect CHS differs from lysosomal storage diseases, where defects in degradation of proteins or lipids often result in a dramatic increase in the volume of lysosomes/late endosomes (49). Instead, the phenotype of CHS and *beige* is more consistent with a defect in fusion or fission of late endocytic structures, which are now known to be highly dynamic, interconnected organelles (8, 33, 34). Such a fusion defect is also suggested by microscopic and histochemical observations of polymorphonuclear lymphocytes (46), Langerhans cells (50), and EBV-transformed cells (47). Therefore, proteins that affect fusion between specific membranes, such as small GTP-binding proteins, are candidates for the gene products affected by the CHS or *beige* mutations. Indeed, changes in the level of expression of rab proteins have been shown to affect the size and cellular localization of the endocytic vesicles they associate with, and overexpression of some rab proteins can generate

large perinuclear organelles (51). Thus, it is of interest that the distribution of rab 5, which associates specifically with early endosomes (35), is the same in both the mutant and control cells. Rab 7, which associates with late endosomes (35), is present on some of the giant organelles, but otherwise its distribution appears to be normal as well. So far, no rabs have been identified that bind to mature lysosomes. Given our qualitative results, it will be informative to test the expression of other rab proteins in *beige* and CHS.

A third conclusion from our results is that the murine *beige* and the human CHS defects cannot be distinguished on the basis of any of the criteria employed here. The distribution of marker proteins, the acidity of the giant lysosomes, their intracellular distribution, the uptake characteristics, and the degradation of ligands are all affected similarly by the mouse and human mutations. Our data therefore support the long-held view that homologous genes are affected in *beige* and CHS. Furthermore, our data suggest a number of assays that can be used in genetic complementation studies, towards identifying the CHS gene.

One of the perplexing aspects of CHS is that secretory granules are affected in some cell types such as granular leukocytes, while endocytic organelles are affected in other cells, like the fibroblasts studied here. That these two types of organelles are affected by the same mutations indicates that they have common components. Indeed, a number of similarities have been observed between lysosomes and secretory granules. Both are acidic organelles, and proteins designated to them are separated from constitutively secreted proteins by sorting into clathrin-coated regions of the *trans*-Golgi network (52). Furthermore, there are a number of specialized cases where secretory functions and lysosomal functions are performed by the same organelles. During bone restructuring, osteoclasts form a tight intercellular space into which they secrete lysosomal enzymes (53). In neutrophils, azurophilic granules fuse with the membrane of the phagosome in a manner that closely resembles an intracellular secretory process, and under certain triggering conditions these granules are capable of direct fusion with the plasma membrane (54). Finally, cytotoxic lymphocytes and natural killer cells contain specialized granules with a cortical domain that resembles late endosomes or lysosomes, and an inner core of secretory proteins. These granules are discharged after binding to an appropriate target cell during cell-mediated cytotoxicity. In cytotoxic lymphocytes, and perhaps in other leukocytes as well, regulated secretory granules appear to be especially similar to lysosomes. This may explain why the effects of CHS are so prominent in leukocytes: secretory granules in these cells may share with lysosomes a protein responsible for regulating their intracellular distribution or their fusion activity. If this view is correct, the affected protein must be much more important for secretory function than for endocytic traffic and degradative function, since the latter is relatively unperturbed by the CHS defect, while the former results in the major clinical manifestations of the disorder.

We thank Delores Johnson and Dr. G. McIntyre for help with a number of the experiments. We also thank Drs. A. Balber, J. Dawson, and B. Sodiek, and members of our group for helpful comments and suggestions throughout.

This work was supported by grants from the American Cancer Society and the Arthritis Foundation. J. K. Burkhardt was a recipient of an Irvington Institute fellowship.

Address correspondence to Dr. Yair Argon, Department of Immunology, Duke Medical Center, Durham, NC 27710. Janis K. Burkhardt's present address is European Molecular Biology Laboratory, Meyerhofstr. 1, D-69012 Heidelberg, Germany.

Received for publication 16 June 1993.

References

1. White, J.G., and C.C. Clawson. 1980. The Chediak-Higashi syndrome: the nature of the giant neutrophil granules and their interactions with cytoplasm and foreign particulates. *Am. J. Pathol.* 98:151.
2. Hargis, A.M., and D.J. Prieur. 1985. Light and electron microscopy of hepatocytes of cats with Chediak-Higashi syndrome. *Am. J. Med. Genet.* 22:659.
3. Penner, J.D., and D.J. Prieur. 1987. Interspecific genetic complementation analysis with fibroblasts from humans and four species of animals with Chediak-Higashi syndrome. *Am. J. Med. Genet.* 28:455.
4. Menard, M., and K.M. Meyers. 1988. Storage pool deficiency in cattle with the Chediak-Higashi syndrome results from an absence of dense granule precursors in their megakaryocytes. *Blood.* 72:1726.
5. Bennett, J.M., R.S. Blume, and S.M. Wolff. 1969. Characterization and significance of abnormal leukocyte granules in the beige mouse: a possible homologue for Chediak-Higashi aleutian trait. *J. Lab. Clin. Med.* 73:235.
6. Oliver, C., and E. Essner. 1973. Distribution of anomalous lysosomes in the beige mouse, a homologue of Chediak-Higashi syndrome. *J. Histochem. Cytochem.* 21:218.
7. Bejaoui, M., F. Veber, D. Girault, C. Gaud, S. Blanche, C. Griscelli, and A. Fischer. 1989. The accelerated phase of

Chediak-Higashi syndrome. *Arch. Fr. Pediatr.* 46:733.
8. Kimball, H.R., G.H. Ford, and S.M. Wolff. 1975. Lysosomal enzymes in normal and Chediak-Higashi blood leukocytes. *J. Lab. Clin. Med.* 86:616.
9. Boxer, L.A., D.F. Albertini, R.L. Baehner, and J.M. Oliver. 1979. Impaired microtubule assembly and polymorphonuclear leucocyte function in the Chediak-Higashi syndrome correctable by ascorbic acid. *Br. J. Haematol.* 43:207.
10. Orn, A., E.M. Hakansson, M. Gidlund, U. Ramstedt, I. Axberg, H. Wigzell, and L.G. Lundin. 1982. Pigment mutations in the mouse which also affect lysosomal functions lead to suppressed natural killer cell activity. *Scan. J. Immunol.* 15:305.
11. Komiyama, A., H. Saitoh, M. Yamazaki, H. Kawai, Y. Miyagawa, T. Akabane, M. Ichikawa, and H. Shigematsu. 1986. Hyperactive phagocytosis by circulating neutrophils and monocytes in Chediak-Higashi syndrome. *Scand. J. Haematol.* 37:162.
12. Ganz, T., J.A. Metcalf, J.I. Gallin, L.A. Boxer, and R.I. Lehrer. 1988. Microbicidal/cytotoxic proteins of neutrophils are deficient in two disorders: Chediak-Higashi syndrome and "specific" granule deficiency. *J. Clin. Invest.* 82:552.
13. Roder, J.C., M.-L. Hohmann-Matthes, W. Domzig, and H. Wigzell. 1979. The beige mutation in the mouse. II. Selectivity of the natural killer (NK) cell defect. *J. Immunol.* 123:2174.
14. Mellman, I., R. Fuchs, and A. Helenius. 1986. Acidification of the endocytic and exocytic pathways. *Annu. Rev. Biochem.* 55:663.
15. Seeman, P.M., and G.E. Palade. 1967. Acid phosphatase localization in rabbit eosinophils. *J. Cell Biol.* 34:745.
16. Peters, C., M. Braun, B. Weber, M. Wendland, B. Schmidt, R. Pohlman, A. Waheed, and K. von Figura. 1990. Targeting of a lysosomal membrane protein: a tyrosine-containing endocytosis signal in the cytoplasmic tail of lysosomal acid phosphatase is necessary and sufficient for targeting to lysosomes. *EMBO (Eur. Mol. Biol. Organ.) J.* 9:3497.
17. Bleil, J.D., and M.S. Bretscher. 1982. Transferrin receptor and its recycling in HeLa cells. *EMBO (Eur. Mol. Biol. Organ.) J.* 1:351.
18. Griffiths, G., B. Hoflack, K. Simons, I. Mellman, and S. Kornfeld. 1988. The mannose-6-phosphate receptor and the biogenesis of lysosomes. *Cell.* 53:329.
19. Lewis, V., S.A. Green, M. Marsh, P. Vihko, A. Helenius, and I. Mellman. 1985. Glycoproteins of the lysosomal membrane. *J. Cell Biol.* 100:1839.
20. Chen, J.W., T.L. Murphy, M.C. Willingham, I. Pastan, and J.T. August. 1985. Identification of two lysosomal membrane glycoproteins. *J. Cell Biol.* 101:85.
21. Gruenberg, J., G. Griffiths, and K.E. Howell. 1989. Characterization of the early endosome and putative endocytic carrier vesicles in vivo and with an assay of vesicle fusion in vitro. *J. Cell Biol.* 108:1301.
22. Dunn, W.A., A.L. Hubbard, and N.N.J. Aronson. 1980. Low temperature selectively inhibits fusion between pinocytic vesicles and lysosomes during heterophagy of 125I-asialofetuin by the perfused rat liver. *J. Biol. Chem.* 255:5971.
23. Zerial, M., R. Parton, P. Chavrier, and R. Frank. 1992. Localization of rab family members in animal cells. *Methods Enzymol.* 219:398.
24. Lyerla, T.A., S.K. Gross, T.B. Shea, P.F. Daniel, and R.H. McCluer. 1987. Biochemical and morphological characterization of primary kidney cell cultures from beige mutant mice. *Cell Tissue Res.* 250:627.
25. Dul, J., O.R. Burrone, and Y. Argon. 1992. Substitution of His for the conserved Tyr/Phe87 in an immunoglobulin light chain creates a conditional non-secreted mutant. *J. Immunol.* 149:1927.
26. Shau, H., and J.R. Dawson. 1985. Identification and purification of NK cells with lysosomotropic vital stains: correlation of lysosome content with NK activity. *J. Immunol.* 135:137.
27. Slot, J.W., and H.W. Geuze. 1985. A new method of preparing gold probes for multiple-labeling cytochemistry. *Eur. J. Cell Biol.* 38:87.
28. Burkhardt, J.K., S. Hester, C.K. Lapham, and Y. Argon. 1990. The lytic granules of natural killer cells are dual-function organelles combining secretory and pre-lysosomal compartments. *J. Cell Biol.* 111:2327.
29. Wiest, D.L., J.K. Burkhardt, S. Hester, M. Hortsch, D. Meyer, and Y. Argon. 1990. Membrane biogenesis during B cell differentiation: most endoplasmic reticulum proteins are expressed coordinately. *J. Cell Biol.* 110:1501.
30. Moncino, M.D., P.A. Roche, and S.V. Pizzo. 1991. Characterization of human alpha 2-macroglobulin monomers obtained by reduction with dithiothreitol. *Biochemistry.* 30:1545.
31. Maxfield, F.R., J. Schlessinger, Y. Schechter, I. Pastan, and M.C. Willingham. 1978. Collection of insulin, EGF and α2-macroglobulin in the same patches on the surface of cultured fibroblasts and common internalization. *Cell.* 14:805.
32. Anderson, R.G.W., J.R. Falck, J.L. Goldstein, and M.S. Brown. 1984. Visualization of acidic organelles in intact cells by electron microscopy. *Proc. Natl. Acad. Sci. USA.* 81:4838.
33. Kornfeld, S., and J. Mellman. 1989. The biogenesis of lysosomes. *Annu. Rev. Cell Biol.* 5:483.
34. Lippincott-Schwartz, J., and D.M. Fambrough. 1986. Lysosomal membrane dynamics: structure and interorganellar movement of a major lysosomal membrane glycoprotein. *J. Cell Biol.* 102:1593.
35. Chavrier, P., R.G. Parton, H.P. Hauri, K. Simons, and M. Zerial. 1990. Localization of low molecular weight GTP binding proteins to exocytic and endocytic compartments. *Cell.* 62:317.
36. Bucci, C., R.G. Parton, I.H. Mather, H. Stunnenberg, K. Simons, B. Hoflack, and M. Zerial. 1992. The small GTPase rab5 functions as a regulatory factor in the early endocytic pathway. *Cell.* 70:715.
37. Green, S.A., K.-P. Zimmer, G. Griffiths, and I. Mellman. 1987. Kinetics of intracellular transport and sorting of lysosomal membrane and plasma membrane proteins. *J. Cell Biol.* 105: 1227.
38. Hammel, I., A.M. Dvorak, and S.J. Galli. 1987. Defective cytoplasmic granule formation. I. Abnormalities affecting tissue mast cells and pancreatic acinar cells of beige mice. *Lab. Invest.* 56:321.
39. Mizushima, W., M. Eguchi, H. Sakakibara, K. Sugita, T. Furukawa, M. Kanagawa, T. Suda, M. Yoshida, Y. Miura, and J. Matsui. 1990. Electron microscopic cytochemistry of pseudo-Chediak-Higashi granules in 5 cases of AML. *Jpn. J. Clin. Hematology.* 31:799.

39a. Takeuchi, K., H. Wood, and R.T. Swank. 1986. Lysosomal elastase and cathespin G in beige mice. Neutrophils of beige (Chediak-Higashi) mice selectively lack lysosomal elastase and cathespin G. *J. Exp. Med.* 163:665.

40. Mane, S.M., L. Marzella, D.F. Bainton, V.K. Holt, Y. Cha, J.E. Hildreth, and J.T. August. 1989. Purification and characterization of human lysosomal membrane glycoproteins. *Arch. Biochem. Biophys.* 268:360.
41. Renfrew, C.A., and A.L. Hubbard. 1991. Sequential processing of epidermal growth factor in early and late endosomes of rat liver. *J. Biol. Chem.* 266:4348.

42. Rabinowitz, S., H. Horstmann, S. Gordon, and G. Griffiths. 1992. Immunocytochemical characterization of the endocytic and phagolysosomal compartments in peritoneal macrophages. *J. Cell Biol.* 166:95.
43. Harding, C.V., and H.J. Geuze. 1992. Class II MHC molecules are present in macrophage lysosomes and phagolysosomes that function in the phagocytic processing of Listeria monocytogenes for presentation to T cells. *J. Cell Biol.* 119:531.
44. Peters, P.J., J. Borst, V. Oorschot, M. Fukuda, O. Krähenbühl, J. Tschopp, J.W. Slot, and H.J. Geuze. 1991. Cytotoxic T lymphocyte granules are secretory lysosomes, containing both perforin and granzymes. *J. Exp. Med.* 173:1099.
45. DeCourcy, K., and B. Storrie. 1991. Osmotic swelling of endocytic compartments induced by internalized sucrose is restricted to mature lysosomes in cultured mammalian cells. *Exp. Cell Res.* 192:52.
46. Irimajiri, K., I. Iwamoto, K. Kawanishi, K. Tsuji, S. Morita, A. Koyama, H. Hamazaki, F. Horiuchi, A. Horiuchi, T. Akiyama, et al. 1992. Studies on pseudo-Chediak-Higashi granules formation in acute promyelocytic leukemia. *Jpn. J. Clin. Hematology.* 33:1057.
47. Jones, K.L., R.M. Stewart, M. Fowler, M. Fukuda, and R.F. Holcombe. 1992. Chediak-Higashi lymphoblastoid cell lines: granule characteristics and expression of lysosome-associated membrane proteins. *Clin. Immunol. Immunopathol.* 65:219.
48. Miller, A.L., R. Stein, M. Sundsmo, and R.Y. Yeh. 1986. Characterization of lysosomes and lysosomal enzymes from Chediak-Higashi syndrome cultured fibroblasts. *Biochem. J.* 238:589.
49. Dingle, J.T., P.J. Jacques, and I.H. Shaw, editors. 1979. Lysosomes in Applied Biology and Therapeutics. North-Holland Publishing Co., Amsterdam, New York. Oxford. 235–284.
50. Carrillo-Farga, J., G. Gutierrez-Palomera, R. Ruiz-Maldonado, A. Rondan, and S. Antuna. 1990. Giant cytoplasmic granules in Langerhans cells of Chediak-Higashi syndrome. *Am. J. Dermatopathology.* 12:81.
51. Bucci, C., R.G. Parton, I.H. Mather, H. Stunnenberg, K. Simons, B. Hoflack, and M. Zerial. 1992. The small GTPase rab5 functions as a regulatory factor in the early endocytic pathway. *Cell.* 70:715.
52. Pfeffer, S.R., and J.E. Rothman. 1987. Biosynthetic protein transport and sorting by the endoplasmic reticulum and Golgi. *Annu. Rev. Biochem.* 56:829.
53. Baron, R. 1989. Polarity and membrane transport in osteoclasts. *Connect. Tissue Res.* 20:109.
54. Estensen, R.D., J.G. White, and B. Holmes. 1974. Specific degranulation of human polymorphonuclear leukocytes. *Nature (Lond.).* 248:347.